

Synthesis and Characterisation of Electrical and Structural Properties of $Mn_{0.4}Zn_{0.6}La_{0.4}Fe_{1.6}O_4$ Nano Ferrites

Neena Panwar, Atul Thakur, Preeti Thakur*

School of Physics, Shoolini University, Solan H.P.

preetithakur@shooliniuniversity.com

Abstract

Magnetic manganese zinc ferrite powder of the composition $Mn_{0.4}Zn_{0.6}La_{0.4}Fe_{1.6}O_4$ was synthesized via co-precipitation technique. Metallic chlorides of manganese, zinc and iron in which Lanthanum is doped were taken. Sodium hydroxide (NaOH) base was used as precipitant agent. The calcinations were performed at 700°C for 3h and sintering at 900°C. The influence of ferrite synthesis condition, such as Zn/Fe molar ratio, pH value and time was investigated. XRD study confirms the formation of single phase spinel structure in the sample. The calculated particle size is found to be 58nm which is good agreement with same investigated by using SEM. The microstructural evolution and morphological features of obtained transition metal ferrites were studied by scanning electron microscopy (SEM) confirms that Structure of the grains of the sample is ultra small size containing a large number of atoms very small in dimension having between 50- 60 nm. By FTIR we got band spectra near 568 cm^{-1} which shows formation of ferrite. The DC resistivity setup confirms that the resistivity of sample varies as with the temperature, when we increase the temperature it decreases and with the decrease in temperature it increases.

Key words: X-ray diffraction (XRD), Scanning electron microscopy (SEM), Fourier Transformation Infrared Spectroscopy (FTIR), DC resistivity setup.

1 Introduction

Mn-Zn ferrites are soft ferromagnetic materials having low magnetic coercivity, low dielectric constant, high resistivity, high

permeability and little eddy current loss in the high frequency range. Magnetic properties of spinel ferrites are influenced by numerous factors such as microstructure, purity, homogeneity and nonstoichiometry. The concentration of ferrous

and ferric ions and their distribution between the tetrahedral and the octahedral sub-lattices, play a critical role in determining their magnetic and electrical properties [1-2]. $Mn_{0.4}Zn_{0.6}Fe_{1.6}La_{0.4}O_4$ ferrite. It is found that small substitutions of Fe ions by rare earths may favourably influence the magnetic and electrical properties of ferrite and therefore, it is thus possible to obtain a good magnetic material. The primary application, for rare earth ferrite magnets, is the voice coil motors that are a part of computer hard disk drives [3]. One purpose of our investigation is to study the role of rare earth types and concentration on the structural and electrical properties of the investigated samples. Also to find a correlation between the above mentioned properties and the ionic rare earth radii in order to obtain well applicable ferrites.

2 Materials and methods

Nano crystalline La doped Mn-Zn ferrite $Mn_{0.4}Zn_{0.6}Fe_{1.6}La_{0.4}O_4$ using stoichiometric amounts of magnesium chloride $[MnCl_2 \cdot 4H_2O]$, zinc chloride $[ZnCl_2 \cdot 4H_2O]$, anhydrous ferric chloride $[FeCl_3 \cdot H_2O]$ and doping lanthanum chloride $[LaCl_3 \cdot 7H_2O]$ dissolved in distilled water. The neutralization is carried out with sodium hydroxide solution and pH is maintained at 8. The precipitate is thoroughly washed with distilled water, dried, crushed and presintered at $700^\circ C$ for 3h and then sample final sintered at $900^\circ C$. These samples are subjected to X-ray diffraction, SEM,

FT-IR, DC resistivity set up studies and the results are discussed below.

3. Results and discussions

3.1 XRD analysis:

The X-ray diffraction (XRD) measurements were taken on for phase identification and study of preferred orientations a full scan of 2θ (from $20^\circ - 80^\circ$) was carried out. The XRD patterns for $Mn_{0.4}Zn_{0.6}Fe_{1.6}La_{0.4}O_4$ ferrite samples with $x=0.4$ is shown in fig 3.1. This fig shows the positions are relative intensities of various XRD peaks. The observed diffraction lines were found to correspond to those of standard pattern of Manganese ferrite with no

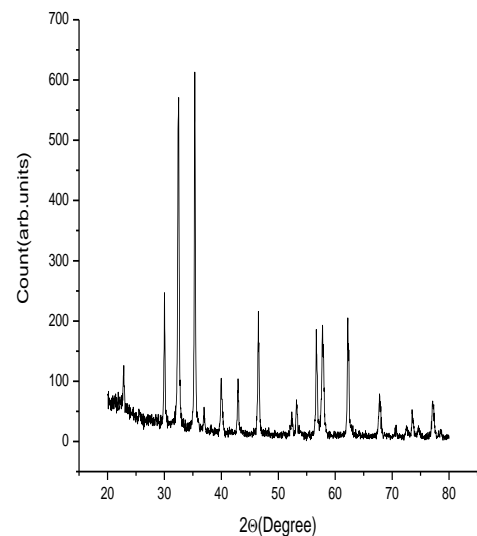


Fig. 3.1 XRD of $Mn_{0.4}Zn_{0.6}Fe_{1.6}La_{0.4}O_4$ sintered at $900^\circ C$

extra lines, indicating thereby that the samples have single phase spinel structure and no unreacted constituents were present in these

samples. Lattice constant 'a' was calculated by using Bragg's law. The lattice constant *a* is calculated from the peaks in X and was found to be 0.462914 for x=0.4. It is found that *a* decreases with increasing La doping concentration for all RE addition samples. These results confirm that La can enter the lattice while keeping the spinel structure unchanged. The decrease in lattice constant may be due to the iron vacancies in these samples. This is expected because the ionic radii of La³⁺(1.15Å) and Fe²⁺(0.83Å) have small difference. The particle size of the samples has been evaluated from the broadening of X- ray diffraction peaks using Scherer's equation [4]. The calculated average particle sizes were found to be for Mn_{0.4}Zn_{0.6}Fe_{1.6}La_{0.4}O₄ ferrites samples is 58nm. This result shows that the synthesized powder has nanocrystallites.

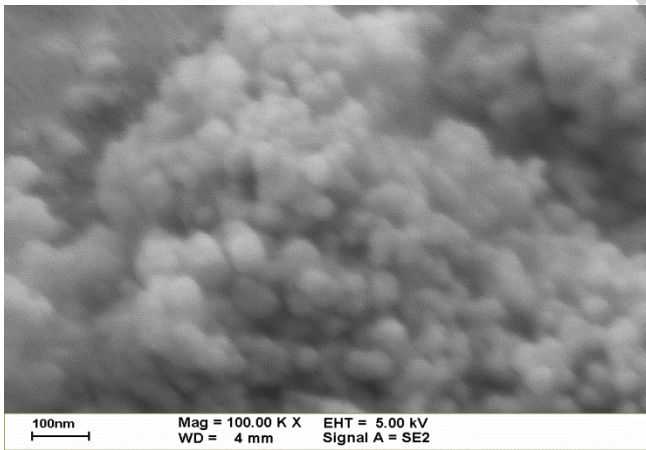
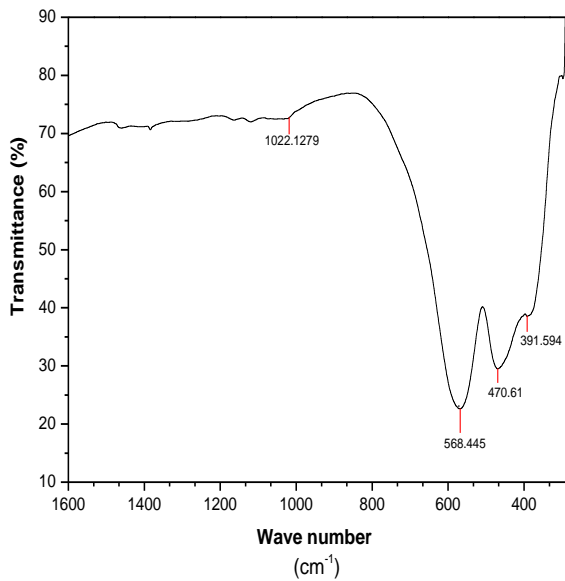


Fig. 3.2 Scanning Electron microscope of Mn_{0.4}Zn_{0.6}Fe_{1.6}La_{0.4}O₄ sintered at 900°C

3.2 Scanning Electron Microscopy (SEM) analysis

We have discussed crystal structure (x-ray diffraction), but consider now different level of structure. Microstructure - also affects properties for mechanical and physical interest are strongly influenced by their microstructures, thus their studies are essential in order to understand the property relationship between the processing parameters as well as behaviour of materials when used in practical applications. In present study scanning electron micrographs (SEM) were recorded using JEOL- 7400 FEGSEM &EDS microscope to examine the microstructural features such as grain size, for ferrites Mn_{0.4}Zn_{0.6}Fe_{2-x}La_xO₄ having composition (x=0.4) prepared by co-precipitation method. Fig. 4.2 show the scanning electron micrographs of Mn_{0.4}Zn_{0.6}Fe_{2-x}La_xO₄ ferrites with x=0.4. The micrographs indicate that the samples have almost uniform sized crystallites with a uniform grain growth. The samples prepared by the conventional methods [5] and the other non conventional methods [6] had grain sizes larger than those observed in the present work. Substitution does not affect the grain growth phenomenon significantly. Structure of the grains of the sample is ultra small size containing a large number of atoms very small in dimension having between 50-60 nm. Also there exist some grains of large size but, smallest grain size is in nm.

3.4 Fourier Transform Infrared spectroscopy (FTIR) analysis



In infrared spectroscopy, IR radiation is passed through a sample. Some of the infrared radiation is absorbed by the sample and some of it is passed through (transmitted). The resulting spectrum represents the molecular absorption and transmission, creating a molecular fingerprint of

Fig.3.3 Fourier transforms infrared spectroscopy of $Mn_{0.4}Zn_{0.6}Fe_{1.6}La_{0.4}O_4$ sintered at $900^\circ C$

the sample. Like a fingerprint no two unique molecular structures produce the same infrared spectrum. Fourier transforms infrared spectroscopy (FTIR) spectra of samples were made with PerkinElmer spectrum FTIR spectrophotometer and we took reading ranging from $1600-200\text{ cm}^{-1}$. The IR spectrum of the sintered material shows the typical bands of the support associated to the skeleton of the spinel. It

can be seen from the Fig. 4.3 that the IR spectrum of $Mn_{0.4}Zn_{0.6}Fe_{2-x}La_xO_4$ ferrite with the La content ($x=0.4$) are found to exhibit two bands in the range $300-600\text{ cm}^{-1}$. As seen in these spectra, only strong absorption bands around 500 cm^{-1} and 600 cm^{-1} due to the metal-oxygen bonds are observed [7]. The absorption bands are caused by the metal-oxygen vibrations in octahedral and tetrahedral sites [8].

Two assigned absorption bands appeared around 600 cm^{-1} : ν_1 , which was attributed to stretching vibration of tetrahedral groups $Fe^{3+}-O^{2-}$ and that around 400 cm^{-1} and ν_2 , which was attributed to the octahedral groups complex $Fe^{3+}-O^{2-}$. In the present spectra, band ν_1 appears near 568 cm^{-1} and shifts to lower frequency with La^{3+} addition. The second absorption band ν_2 appears near 470 cm^{-1} and also shifts to lower frequencies with La addition. The differences in frequencies between ν_1 and ν_2 is due to changes in bond length ($Fe^{3+}-O^{2-}$) at octahedral and tetrahedral sites. The band spectra near 568 cm^{-1} show formation of ferrite. All characteristic peaks in FTIR spectrum were analysed and confirmed the formation of ferrite phase[9].

4.5 DC resistivity

The value of dc resistivity for $Mn_{0.4}Zn_{0.6}La_{0.4}Fe_{1.6}O_4$ ferrites obtained by co-precipitation method is found to be of the order of 10^7 cm . This shows that dc resistivity obtained in co precipitation method is greater as compared to conventionally ($\approx 10^2\Omega m$) normal prepared Mn-Zn ferrites [10]. The higher value of dc resistivity

is because of the stoichiometric compositions, better crystal structures and the improved

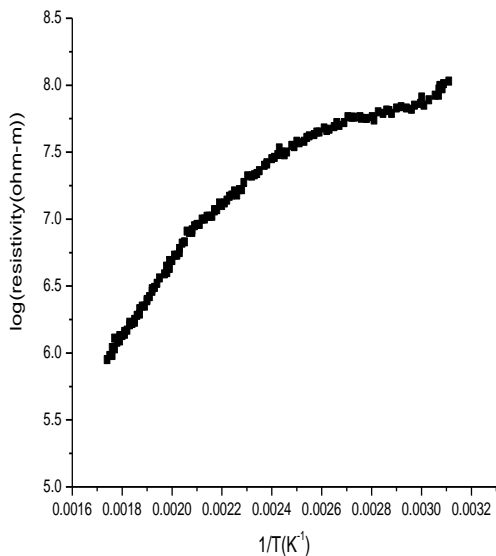


Fig.4.4 variation of log resistivity (ohm-m) of sample of $Mn_{0.4}Zn_{0.6}Fe_{1.6}La_{0.4}O_4$ sintered at $900^{\circ}C$ with $1/T (K^{-1})$

nano structures obtained by the co-precipitation method. Samples with smaller grains contain

Temperature(K)	Resistance	Resistivity (ohm-m)
41	2353000	8.7×10^7
101	1099000	4.07×10^7
200	198400	7.3×10^6
300	19300	7.15×10^5

greater number of grain boundaries. The grain boundary is a region of mismatch between the energy states of the adjacent grain and hence acts as a barrier to flow of electrons and therefore decrease the conductivity. Another advantage of small grain size is that it helps in reducing Fe^{2+} ion as oxygen moves faster in small grain thus keeping iron in Fe^{3+} state. In conventional ceramic

method, the sintering temperature being higher, the grains are relatively bigger. Further the, extensive ball milling required in the conventional method may result in loss of few grains of the introduction of impurities. This would result in non-stoichiometric and non homogenous sample.

In co-precipitation method, these possibilities being negligible, higher resistivity of the prepared samples is therefore expected. At low temperature the value of resistivity of the sample is high and at high temperature the value of resistivity of the sample is low. The curie temperature of the material i.e., is that above material shows paramagnetic properties and below which the materials are ferromagnetic. $T_c = 432K$ which is calculated from Fig.3.4 We have shown in following table calculated resistivity at different temperature as:

From above table it is concluded that the resistivity of sample varies as with the temperature, when we increase the temperature it decreases and with the decrease in temperature it increases. Activation energy, E_p was calculated from the slope of the graph given in Fig 3.4. It is found that the value of activation energy in the ferrimagnetic region is lower than that of the paramagnetic region. The lower activation energy in the ferromagnetic region is attributed to the magnetic spin disordering [11] due to decrease in the concentration of current carriers [12], while the change in activation energy is attributed to the

change in conduction mechanism[13] and (Singh and Sud, 2000), Activation energy for the sample is found to be 0.61688 eV, which indicates that ferrite formed is p-type semiconductor. The increase in resistivity is also attributed to the p-type conductivity, which increases the activation energy on the basis of Verwey conduction mechanism [15].

4 Conclusions

XRD study confirms the formation of single phase spinel structure in the sample. The calculated particle size is found to be 58nm which is good agreement with same investigated by using SEM.

SEM study confirms that the synthesized ferrites have almost uniform sized crystallites with a uniform grain growth. Substitution does not affect the grain growth phenomenon significantly. Structure of the grains of the sample is ultra small size containing a large number of atoms very small in dimension having between 50- 60 nm.

The results obtained from infrared spectral studies of $Mn_{0.4}Zn_{0.6}Fe_{1.6}La_{0.4}O_4$ ferrite nano particle show two significant absorption bands. The position of absorption bands are compositional dependent, whose dependence could be attributed to the variation in metal - oxygen band distances.

High values of DC resistivity in the range of $10^7 \Omega m$ are obtained for the Lanthanum substituted Mn-Zn ferrites. Power losses due to

eddy currents are much reduced in this ferrite and are therefore well suited for microwave frequencies applications. The Activation energy the sample is found to be 0.61688 eV, which indicates that ferrite formed is Combustion Route p-type semiconductor. It is observed that the DC resistivity can be sensitively controlled by Lanthanum substitution. The resistivity of sample varies as with the temperature, when we increase the temperature it decreases and with the decrease in temperature it increases.

Acknowledgement

I would like to thanks Rikhi chand FTIR lab SAIF PU Chandigarh, Sumit bhardwaj and Dev Raj Thakur XRD lab NIIT Hamirpur for providing us XRD and FTIR facilities for sample characterisation.

References

1. Yoo, H.I. and Tuller, H.L. (1988) *J. Phys. Chem. Solids*, 9 (7):761.
2. Rezlescu, N., Rezlescu, E. (1993) *Solid State Commun.* 88(2):139.
3. Soohoo, R.F. (1985) *Microwave Magnetics*, Harper and Row, New York.
4. Cullity, B.D. (1978) *Elements of X-ray Diffraction*, Addison-Wesley, Reading, MA.
5. Bermejo, E., Mercier, T.I.C. and Quartan, M. (1995) *J. Amm. Ceram. Soc.*78 (2): 365.
6. Johnson, D.W. (1974) *J. Amm. Ceram. Bull.* 53(2): 163.
7. Durán, P., Tartaj, J., Rubio, F., Moure, C. and Peña, O. (2005) Synthesis and sintering behavior of spinel-type $Co_xNiMn_{2-x}O_4$ ($0.2 < x < 1.2$) prepared by the ethylene glycol-metal322: 866 – 871.

8. Sertkol, M., Koseoglu, Y., Baykal, A., Kavas, H. and Toprak, M. S. (2010) Synthesis and Magnetic Characterization of $Zn_{0.7}Ni_{0.3}Fe_2O_4$ Nanoparticles via Microwave-assisted Combustion Route *Journal of Magnetism and Magnetic Materials* 322: 866 – 871.
9. Muthuroni, S., Balaji, M., Gautam, S., Keun, Hwachae, Song, J.H., Pathinettam, Padiyan D. and Asokan, K. (2010) Magnetic and humidity sensing properties of nano-structured $Cu_xCo_{1-x}Fe_2O_4$ synthesized by auto combustion technique. *J. Mat. MAT. sci.*, pp. 1-12.
10. Thakur, A. and Singh, M. (2003) *J. Ceramic international* 29: 505-511
11. Barerner, K., Mandal, P. and Helmolt, R.V. (2001) *Phys. Stat. Sol. (b)* 223: 811–820.
12. Baszsyński, J. (1969) *J. Acta Phys. Polym.* 35: 631.
13. Murthy, V.R.K. and Sobhandri, J. (1977) *Phys. Stat. Sol. (A)* 38 : 647.
14. Singh, M. and Sud, S.P. (2000) *J. Mater. Sci. Eng. B* 83: 181.
15. Verwey, E.J.W., Haaijman, P.W., Romeyn, F.C. and Oosterhout, van, G.W. (1950) *Philips Res. Rep.* 5: 173–187.